A MODELING STUDY: ON THE INFLUENCE OF HIGH FREQUENCY OCEAN-ATMOSPHERE INTERACTIONS OVER INTRA-SEASONAL OSCILLATIONS (DURING THE EL NINO 1997-98)

Enver M. A. Ramirez Gutierrez[1] & Iracema F. A. Cavalcanti

Centro de Previsão de Tempo e Estudos Climáticos (CPTEC)
Instituto Nacional de Pesquisas Espaciais (INPE), Brasil

1. INTRODUCTION

The efficiency of Atmospheric General Circulation Models (AGCMs) to represent intra-seasonal oscillations has been analysed in several studies (e.g. Slingo et al., 1996; Sperber et al., 1996). Slingo (1996) working with fifteen, state of the art, AGCMs showed that even when it is possible to find energy at intra-seasonal scales, in some cases the sources of that energy does not have an observational counterpart; and in other group the oscillations obtained show periods shorter than the observed.

On the other hand, Coupled General Circulation Models (CGCMs) still have problems to correctly represent the basic (mean) state (Inness 2002, Zheng et al., 2004), which is believed to interact with intra-seasonal scales (Zheng et al., 2004; Slingo et al., 1996; Sperber et al., 1996) and to define some observed characteristics. Among the intra-seasonal oscillations, the MJO is the dominant one (Wheeler and Kiladis, 1999) and despite extensive studies, the mechanisms by which the MJO, originates, amplifies, and then decay, are still an open question (Zhang 2005; ECMWF Workshop 2003). Much of the nowaday work is concentrated into finding a theory able to quantitatively reproduce the eastward propagation, wavenumber/frequency dependency and time lead/lag relationships between variables.

Theoretical work by Wang and Xie (1998) suggested that a MJO like mode could appear if ocean-atmosphere coupling is considered. However, other studies, consider the interaction with the ocean only as a modulating mechanism (Zheng et al., 2004).

In the present study, convectively coupled equatorial waves (Wheeler and Kiladis, 1999), emphasizing the MJO and the Rossby wave were studied, by coupling the Quasiequilibrium Tropical Circulation Model (QTCM) with a Slab Mixed Layer Ocean Model (SMLOM). The SMLOM evolution was parameterized as a function of the Heat Fluxes Budget, and the depth used is consistent with a diurnal ocean mixed layer. As in the heat flux balance, the net solar radiation is also considered and a model representation of the diurnal cycle is included in the time evolution correction of the specified SST.

1 *Corresponding author address*: Enver M. A. Ramírez Gutierrez Centro de Previsão e Estudos Climáticos – Instituto Nacional de Pesquisas Espaciais. email: eramirez@cptec.inpe.br

2. METHODOLOGY

2.1 Atmospheric Model (QTCM)

QTCM is an intermediate complexity tropical circulation model; that uses approximations related to the quasi-equilibrium in the convective parameterizations. These assumptions, under certain approximations, can be used to generate analytical solutions for the large-scale fluxes (Neelin et al., 2000). These solutions are used to construct an adapted numerical scheme, that responds for the interaction of the convection with the large-scale dynamics. The method is accurate for convective regions, within a radius of 25 degrees, and highly truncated outside of these regions. This method also combines the simplicity of analytical solutions, without the necessity of simplifying the non-linearity (Neelin and Yu 1994; Yu and Neelin 1997; Neelin and Zeng 2000; Zeng et al., 2000). To obtain more accurate solutions, intermediate physical process parameterizations were included in the model, as for example a radiative pack (Chou and Neelin 1996) and a surface model (Zeng et al., 2000). The convective scheme follows a modification of Betts and Miller parameterization (1986; 1993).

2.2 High frequency ocean-atmosphere coupling

To study the effect of the inclusion of a dynamic SST on the intra-seasonal oscillations and the MJO, a high frequency ocean-atmosphere coupling with a diurnal slab mixed layer ocean model (SMLOM) was implemented in the standard QTCM. The SST time evolution correction is parameterized as a function of heat flux balance and the coupling carried out at the atmospheric integration time step (each twenty minutes). In this way, corrections at periods shorter than one day are allowed. In the present study, a high frequency correction to the daily SST (interpolated from monthly observed values) was implemented without using intra-seasonal relaxation damping. For comparison purposes, three nine-year simulations were performed; the first one is a control run denominated RT; in the second one (RT_DCPLS) the high frequency coupling was implemented in an equatorial pacific area (150E-135W; 3.75S-3.75N); whereas in the third one (RT2_DCPLS) the high frequency coupling were implemented over all the equatorial oceans in a radius of 3.75 degrees around the equator.

3. ANALYSIS

3.1 Time Series - Heat Fluxes:

Table 1 shows the Net Heat Fluxes, for different El Nino regions, and also the individual components of this balance in terms of percentage. The Heat Flux is defined as positive toward the ocean, so any positive balance implies in a gain of energy by the ocean. Although precipitation was not considered in the implemented parameterization, it is shown for comparison purposes.

The short wave radiation has the greatest contribution to the heat fluxes gain (20%). Meanwhile the evaporation has the greatest negative contribution (4-9%). Other terms that have a relative importance are the Long Wave Radiation (36%) and the counter radiation (32%), but as In the QTCM the second is function of the first, and they always act together, the net effect is to cancel each other, leaving a negative Long wave contribution of around 4%. So in the tropical ocean, the effect of the Net Heat Fluxes is to introduce energy into the ocean. It can also be noticed, that the amplitude of the Heat budget increases toward the East, being greater in the El Nino 1+2 region (Table 1). This agrees quite well with the results of Battisti (1988).

Figure 1, shows the relationship between the Heat Flux Budget and the SST Tendency for the different El Nino regions. (El Nino 3.4 was not displayed as it does not shown noticeable differences with respect to El Nino 3). It can be noticed that there is a good correspondence between SST tendency and Heat Fluxes, and that the Heat Flux curve precedes the SST tendency. The smooth variation in the central and west Pacific when compared with the East Pacific region can be associated with more intense temperature gradients in the El Nino 1+2.

3.2 Time Series - OLR:

To make the analysis of OLR, the area limited between 120E-180E, 10S-10N was chosen. Slingo et al. (1996); Sperber et al. (1996) found that, in general, models have problems to represent the propagation of intra-seasonal signals through this region. As can be seen in Figure 2, the total OLR appears to be less influenced by the implementation of the high frequency coupling (see continuous curve), but it is possible to note that there is an intensification of the intra-seasonal variability in special during the El Nino 1997/98 (dotted line). Figure 3 shows a zoom of the intra-seasonal variance (continuous line). The variability increase of the intra-seasonal component is evident, in the cases where the coupling was implemented (dashed line). The cumulative variance (dotted line) for the control experiment (RT) shows that two events caused an increment in the OLR variability, the first one at the beginning of 1997, while the second at the beginning of 1998. The number of events that altered the variability, in the case of the RT_DCPLS experiment, were also two, however with a shift in time (First one at around mid 1997, and the second one at the beginning of 1998). For

the case of the RT2_DCPLS experiment, in which the high frequency coupling was implemented over all the oceans, three most significative events in terms of variability were recorded. They coincide with the occurrence of the events recorded in the two previously described experiments. The variability of the total OLR was not substantially altered, which suggests that a possible energy redistribution of the energy might be happened. Given that the forcing is introducing high frequency correction, it would imply in a mechanism to convert high frequency to intra-seasonal variability.

With the inclusion of the high frequency coupling, the variability of the total OLR was not modified, remaining almost constant in the three experiments. Differences can be noted (around 10 W/m^2) but only in some years. Thus the coupling acts mainly over the intra-seasonal variability, which is also consistent with other studies (see Flatau et al. 1997). The applicability of these results, has a potential, not only to a better understanding of El Nino and the MJO, but also in terms of extended weather forecast, because it could be used in the scope of ensemble forecast in which, an element with the high frequency coupling could represent a scenario of intensified intra-seasonal variability.

3.3 Spectral Filtering (SF)

Analysis of the MJO (Figure 4) for all the experiments (RT, RT_DCPLS and RT2_DCPLS) shows that it tends to amplify as the Southern Hemisphere Summer is established. Comparisons of the three experiments reveal that in both the RT and RT_DCPLS simulations favorable-to-convection phase of the MJO (dark shaded) were not found eastward of the International Date Line. However the amplitude of the oscillations are increased in RT_DCPLS. On the contrary, favorable signals eastward of the date line are found in the RT2_DCPLS simulation (coupling implemented over all the oceans). This could suggest that the inclusion of the coupling not only contributes to the amplification of the signal, but also to its propagation, and in this case over the Indian to West Pacific oceans, a generally problematic region for the numerical models (Sperber et al. 1996). A further inspection of these figures, also reveals, that the phase speed of the MJO (4-6 m/s) is closer to the observations in the case of the RT2_DCPLS simulation (3.8 m/s) with zonal wavenumber varying from 1-2. In RT experiment is 2.3 m/s and in RT_DCPLS simulations is 3.6 m/s (these two with zonal wavenumber 1). So this analysis also reveals that the intra-seasonal oscillation, specifically the MJO, is amplified with the inclusion of the coupling.

3.4 Terciles:

Until now, it has been shown, that in some isolated regions the intra-seasonal variability were amplified. With the aim to characterize the spatial distribution of the impact of the high frequency coupling, in special to separate the effect of it over the different components of the intra-seasonal variability, a classification in Terciles

1338

was applied to both the MJO and the Rossby wave and for all the simulations.

Two classifications were applied, the Direct Count (DC), and the Indirect Count (IC). DC consists into finding thresholds that limit each wave of the RT simulation in three categories bellow, normal and above normal. With these thresholds, by means of a simple count, the same wave is classified, but for the experimental simulations (RT_DCPLS and RT2_DCPLS independently). This classification was performed for each grid point within the tropical region (20S-20N). Thus, the spatial distribution of the effect of the coupling on the same wave is obtained. The results are presented in terms of percentages.

For the IC, the amplitude squared of the MJO, was used to classify the amplitude squared of the Rossby for the same simulation. IC allows us to identify, how is the distribution of the energy between MJO and Rossby (which displays opposed phase speed) and if this distribution is modified by the implementation of the high frequency coupling, owing to a preferentially amplification of one of these modes.

The interpretation of Figures 5-7 is more clear if the central panel (normal) is observed first. No-shading indicate regions in which the high frequency coupling did not change the distribution of events. Bluish colors represent regions in which the number of events diminishes with respect to the normal, representing an increase of extreme events. Finally reddish colors represent regions in which an increase of events within the normal category was recorded (A reduction of extreme events).

Figure 5 shows that in effect an amplification of both intra-seasonal components exists when high frequency coupling is implemented. Meanwhile Figure 6,7 adds that a preference for eastward modes amplification does exist. It explains, in some manner, the improvements in terms of phase speed propagation across the Maritime Continent when the coupling is included.

4. FINAL COMMENTS

In the present work, the QTCM model (an intermediate complexity tropical circulation) is used to test the impact of a high frequency ocean-atmosphere coupling (representative of the diurnal cycle) into the intra-seasonal variability. QTCM is a non-linear, primitive equation based model that makes use of approximations related to the Quasi-Equilibrium to construct a numerical scheme highly accurated around Tropical Convective Regions and highly truncated out of them. In this way the role of Tropical Convection as tropical forcing is highlighted. It was noticeable that favorable-to-convection MJO signals to the east of the International Date Line were more pronounced when the coupling was included. It was also shown, with Terciles analysis that although coupling amplify both intra-seasonal components (MJO and Rossby), Indirect Count shows that coupling amplifies preferentially the MJO.

The present study is in agreement with some previous results (Flatau et al., 1997; Waliser et al., 1999). However, it goes further by showing that from all the intra-seasonal components, the MJO is the preferentially amplified (by the high frequency coupling). Although the exact mechanisms by which this occurs are still not fully understood, it is suggested that there is an energy transfer from high frequency to intra-seasonal variability. This suggestion was discussed in Ramirez Gutierrez and Cavalcanti 2005. This might be happening through the Quasi-Equilibrium adjustment, as a modification of the temperature reference profile by the boundary layer evolution and also by the downdrafts are included. The coupling acts directly over the boundary layer, correcting the surface temperature, and in this way, the moist static stability.

Several models have shown an intra-seasonal Energy Partition that favors the Rossby instead of the MJO (Slingo et al., 1996; Sperber et al., 1996). It must be desired to investigate if the coupling applied in the present study is able to correct this common mistake.

References

Battisti. D. S., 1988: Dynamics and Thermodynamics of a Warming Event in a Coupled Tropical Atmosphere-Ocean Model. *J. Atmos. Sci.*, **45,** 2889-2919.

Betts A. K., e Miller M. J., 1986: A new convective adjustment scheme. Part II: Single column test using GATE wave, BOMEX, ATEX and artic air-mass data sets. *Quarterly Journal of the Royal Meteorological Society*, **112,** 693-709.

Betts A. K., e Miller M. J., 1993: The Betts-Miller scheme: the Representation of Cumulus Convection in Numerical Models of the atmosphere. *Amer. Meteor. Soc., Meteor, Mon.* **24**, p.107-121, 1993.

Chou, C. And J. D. Neelin., 1996:, Linearization of a longwave radiation scheme for intermediate tropical atmospheric models. *J. Geophys. Res.,* **101**, 15,129-15,145.

Flatau M., P. J. Flatau, P. Phoebus, P. P. Niiler., 1997: The feedback between equatorial convection and local radiative and evaporative processes: the implications for intra-seasonal oscillations. *Journal of the Atmospheric Science*, **54,** p.2373-2386.

Inness P. M., 2002: Representation of the Madden-Julian Oscillation in General Circulation Models. *Thesis for Doctor of Philosophy. Reading University UK*, 2002.

Neelin, J. D., and J.-Y. Yu., 1994: Models of tropical variability under convective adjustment and the Madden-Julian oscillation. Part I: Analytical results. *Journal of the Atmospheric Science*, **51,** 1876-1894.

Neelin, J. D., and N. Zeng., 2000: A Quasi-Equilibrium Tropical Circulation Model - Formulation. *J. Atmos. Sci.,* **57,** 1741-1766.

Ramirez Gutierrez, E. M. A., Cavalcanti, I. F.A., 2004: Estudo Preliminar: Comparação das oscilações intrasazonais do MCGA CPTEC/COLA com as ondas das teorias clássicas de Matsuno e Gill. *Anais do XIII Congresso Brasileiro de Meteorologia – XIII CBMET – SBMET*, Fortaleza Ceará.

Ramirez Gutierrez, E. M. A., Cavalcanti, I. F.A., 2005: Um estudo de modelagem sobre: A influência da interação oceano-atmosfera nas oscilações intrasazonais durante o El Niño 1997-98 *Master´s degree Dissertation* , INPE São José dos Campos.

Slingo J. M., Sperber K.R. , J.S. Boyle, J-P. Ceron, M. Dix, B. Dugas, W. Ebisuzaki, J. Fyfe, D. Gregory, J-F. Gueremy, J. Hack, A. Harzallah, P. Inness, A. Kitoh, WK-M. Lau, B. McAvaney, R. Madden, A. Matthews, T.N. Palmer, C-K. Park, D. Randall, N. Renno, 1996: Intra-seasonal oscillations in 15 atmospheric general circulation models: results from an AMIP diagnostic subproject, *Climate Dynamics*, **12,** 325-357.

Sperber K. R., J. M. Slingo, P. M. Inness, W. K-M. Lau, 1996: On the maintenance and initiation of the intra-seasonal oscillation in the NCEP/NCAR reanalysis and the GLA and UKM AMIP simulations. *PCMDI report No 36*.

Waliser, D. E., K. M. Lau, J.-H. Kim., 1999: The influence of the coupled sea surface temperatures on the Madden-Julian Oscillation: A model perturbation experiment. *J. Atmos. Sci.,* **56**, 333-358.

Wang B., e Xie X., 1998: Coupled modes of the warm pool climate system Part I: The role of the air-sea interaction in maintaining the Madden-Julian oscillation. *J. Climate*, **8,** 2118-2135.

Wheeler M. and G. N. Kiladis, 1999: Convectively Coupled Equatorial Waves: Analysis of Clouds and Temperature in the Wavenumber-Frequency domain, *J. Atmos. Sci,* **53**, 374-399.

Yu, J.-Y., e J. D. Neelin, 1997: Analytic approximations for moist convectively adjusted regions. *J. Atmos. Sci.,* **54**, 1054-1063.

Zeng N., J. D. Neelin e C. Chou, 2000: A Quasi-Equilibrium Tropical Circulation Model – Implementation and Simulation. *J. Atmos. Sci.,* **57,** 1767-1796.

Zhang C. e M. J. McPhaden, 2000: Intra-seasonal surface cooling in the equatorial western Pacific. *J. Climate,* **13,** 2261-2276.

Zhang C., 2005: Madden-Julian Oscillation. *Reviews of Geophysics*, **43**, 1-36.

Zhang C., 2003: Structures of the MJO: Implications to its air-sea interactions and dynamics. *Workshop on Intraseasonal Variability with Emphasis on the MJO*, Reading, U.K., ECMWF, p.1-36.

Zheng Y., Waliser D., Stern W., Jones C., 2004: The Role of coupled sea surface temperatures in the simulation of the tropical intra-seasonal oscillation. *J. Climate* **17,** 4109-4134.

	Niño4	Niño3.4	Niño3	Niño1+2
Fn (ºC/d)	0.072	0.11	0.14	0.2
Swd (%)	19.06	20.47	21.35	22.41
Swu (%)	-1.13	-1.2	-1.26	-1.69
Lwd (%)	32.83	32.5	32.6	33.29
Lwu (%)	36.64	-36.20	-36.35	-36.8
Evap (%)	-9.31	-9.15	-8.24	-4.61
Prec (%)	1.48	0.56	0.23	0.13
Fts (%)	-1.0	-0.45	-0.13	-1.176

Table 1. Mean values for all the period of the model integration of Net Heat Flux (Fn) and the percentage of individual contribution (Ramirez Gutierrez and Cavalcanti 2005). The abbreviations are: Swd (short wave downward), Swu (short wave upward), Lwd (Long wave downward), Lwu (Long wave upward), Evap (Evaporation), Prec (Precipitation), and Fts (Sensible Heat Flux).
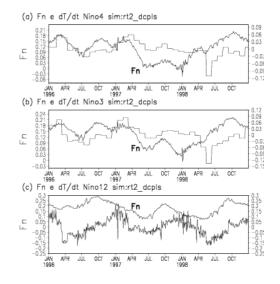

Figure 1. Area averaged mean of the Net Heat Flux and SST tendency for the different regions in which the El Niño is monitored. (a) El Niño4, (b) El Niño 3 and (c) El Niño 1+2.

(a) OLR e OLR_3060 Lon 120 180 Lat −10 10 sim:RT

(b) OLR e OLR_3060 Lon 120 180 Lat −10 10 sim:RT_DCPLS

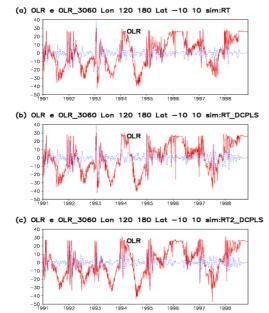(c) OLR e OLR_3060 Lon 120 180 Lat −10 10 sim:RT2_DCPLS

Figure 2. OLR with the period mean excluded (continuous line) and 30-60 days band passed OLR (dotted line). The upper panel (a) corresponds to the RT simulation, while the second (b) and third panel (c), corresponds to the RT_DCPLS and RT2_DCPLS respectively. The time series correspond to an Area average 120E – 180, and 10S – 10N.

(a) OLR_3060 Lon 120 180 Lat −10 10 sim:RT

(b) OLR_3060 Lon 120 180 Lat −10 10 sim:RT_DCPLS
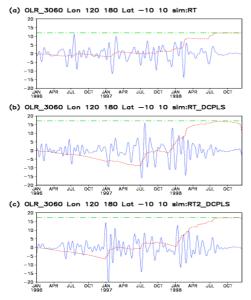
(c) OLR_3060 Lon 120 180 Lat −10 10 sim:RT2_DCPLS

Figure 3. 30-60 days band passed (continuous line), total variance (dashed line) and cumulative variance (dotted line). Again, the upper panel (a) correspond to the RT simulation, while the second (b) and third (c) corresponds to the RT_DCPLS and RT2_DCPLS respectively. Similarly to Figure 2.a, an Area average 120E – 180, and 10S – 10N was used.
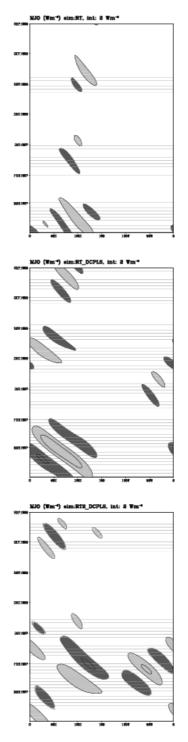

Figure 4. Hovmoller diagrams of the MJO for a) RT; b) RT_DCPLS and c) RT2_DCPLS simulations. The shading interval is 1 W/m2, each wave was averaged in an Equatorial band of 5º around the Equator. The time runs from September 1996 to March 1997.

1341

(a) Abaixo do Normal (%) sim:rt2_dcpls

(b) Normal (%) sim:rt2_dcpls
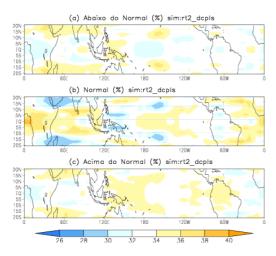
(c) Acima do Normal (%) sim:rt2_dcpls

Figure 5. Spatial Distribution (classified in terciles) of the effect of the high frequency ocean-atmosphere coupling over the OLR-Rossby (RT2_DCPLS simulation) with respect to the OLR-Rossby (RT simulation). Three categories are shown a) Above; b) Normal; c) Below, and for each of them, bluish colors represent points in which the number of events in that category diminishes with respect to the RT simulation. Reddish colors represent regions in which the number in that category increased. Values around 33% (which represent neutrality) are white shading.
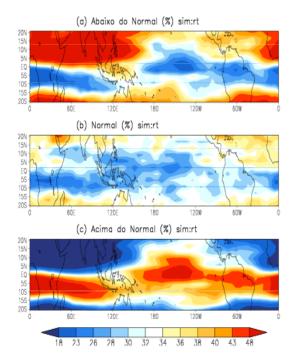

(a) Abaixo do Normal (%) sim:rt

(b) Normal (%) sim:rt

(c) Acima do Normal (%) sim:rt

Figure 6. Spatial Distribution of **IC** (Indirect Count). It represents the effect of the high frequency ocean-atmosphere coupling over the **OLR-Rossby Power** (squared amplitude; RT simulation) with respect to the **OLR-MJO Power** (RT simulation). Three categories are shown a) Above; b) Normal; c) Below, and for each of them, bluish colors represent points in which Rossby waves are less energetic than the MJO. Reddish colors represent regions in which Rossby waves were more energetic than MJO. Values around 33% (which represent neutrality) are white shading.
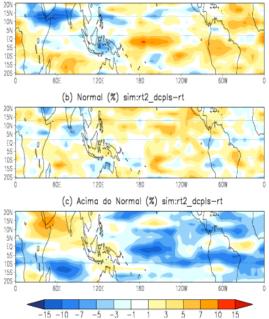

(a) Abaixo do Normal (%) sim:rt2_dcpls−rt

(b) Normal (%) sim:rt2_dcpls−rt

(c) Acima do Normal (%) sim:rt2_dcpls−rt

Figure 7. Spatial Distribution of **IC** (simulation RT2_DCPLS) – **IC** (control run RT) classified in terciles. **IC (RT2_DCPLS)** represents the effect of the high frequency ocean-atmosphere coupling over the **OLR-Rossby Power** (squared amplitude; RT2_DCPLS simulation) with respect to the **OLR-MJO Power** (RT2_DCPLS simulation). Three categories are shown a) Above; b) Normal; c) Below, and for each of them, bluish colors represent points in which **IC** distribution diminishes with respect to the **IC-RT** simulation. Reddish colors represent regions in which **IC** distribution increased with respect to **IC-RT** simulation. Values around 33% (which represent neutrality) are white shading.